NUKLEONIKA 2012;57(4):473–476

ORIGINAL PAPER

High-temperature oxidation resistance in yttrium implanted stainless steel

Marek Barlak, Jerzy Piekoszewski, Zbigniew Werner, Bożena Sartowska, Lech Waliś, Wojciech Starosta, Joachim Kierzek, Ewa Kowalska, Richard A. Wilhelm, Cezary Pochrybniak, Magdalena Woźnica

Abstract. Austenitic AISI 304, 316L and ferritic 430 stainless steels were implanted with yttrium to fluences ranging between 1×10^{15} and 5×10^{17} ions/cm^2. The samples were subjected to oxidation in air at a temperature of 1000°C for a period of 100 h and next examined by stereoscopic optical microscopy (OM), scanning electron microscopy (SEM), energy dispersive X-ray spectrometry (EDX) and Rutherford back scattering spectrometry (RBS). The results obtained with the use of ion implantation are discussed.

Key words: high-temperature oxidation resistance • ion implantation • yttrium

M. Barlak✉, J. Piekoszewski, Z. Werner, E. Kowalska, C. Pochrybniak, M. Woźnica
National Centre for Nuclear Research (NCBJ),
7 Andrzeja Sołtana Str., 05-400 Otwock/Świerk, Poland,
Tel.: +48 22 718 0644, Fax: +48 22 779 3481,
E-mail: barlak@ipj.gov.pl

B. Sartowska, L. Waliś, W. Starosta, J. Kierzek
Institute of Nuclear Chemistry and Technology,
16 Dorodna Str., 03-195 Warsaw, Poland

R. A. Wilhelm
Helmholtz-Zentrum Dresden-Rossendorf,
P. O. Box 51 01 19, D-01314 Dresden, Germany

Received: 7 October 2011
Accepted: 1 March 2012

Introduction

The addition of some amount of oxygen reactive elements like Y and rare earth elements (REE) Ce, La, Er and others into stainless steels or iron chromium alloys improves their oxidation resistance at high temperature.

Although the question of yttrium doping has been investigated since the 80s of the last century [11, 12, 16] and there are numerous methods of incorporation of REE into steel by surface treatment, e.g.: ion implantation, metal organic, chemical vapour deposition, sol-gel coating, pack cementation, screen-printing, molten-salt electrodeposition [1–4, 6–8, 13–15, 17, 18], many questions related to the problem of steel corrosion improvement remain unresolved.

In the present work we intend to use yttrium as an active element which will be incorporated into 304, 316L and 430 stainless steels using conventional ion implantation with a MEVVA type yttrium ion source.

Experimental

Samples

Samples were cut from AISI 304, 316L commercial austenitic stainless steel and 430 ferritic stainless steel in the form of plates of $20 \times 10 \times 1$ mm^3 in size, with roughness of about R_a: 0.1 μm, 0.06 μm and 0.04 μm for 304, 316L and 430 stainless steel, respectively. Before processing, the samples were washed in high purity acetone in an ultrasonic bath.

Processing

Yttrium ions were implanted into steel samples using a MEVVA type implanter with direct beam without mass separation, described in detail elsewhere [5].

To avoid overheating effects, the samples were clamped onto a water-cooled stainless steel plate and the ion current densities were kept below 10 $\mu A/cm^2$, so the substrate temperature did not exceed 200°C. The base pressure in the vacuum chamber was about $2–5 \times 10^{-4}$ Pa.

Ions were implanted at 65 kV acceleration voltage. Nitrogen of 99.9% purity supplied by Air Liquide Polska was used as the implanter working gas. The fluence range was from 1×10^{15} to 5×10^{17} ions/cm^2.

Selected implanted samples were subsequently oxidized at 1000°C for 100 h in air at 50% relative humidity. The heating rate was about 25°C/min and the cooling rate was about 10°C/min.

Characterization

The samples were characterized by stereoscopic optical microscopy (OM), scanning electron microscopy (SEM), energy dispersive X-ray spectroscopy (EDX), and Rutherford back scattering (RBS) examination. The quality of the surface of oxidized samples were examined with the use of a stereoscopic optical microscope. Scanning electron microscopy was used to examine the changes in the morphology of the processed and oxidized sample at magnification ×5000.

Energy dispersive X-ray spectrometry was used for determination of the surface elemental composition.

In order to get insight into the composition of the processed layer, the selected samples were subjected to Rutherford back scattering examination. The energy spectra of back scattered 1.7 MeV He^+ particles, incident perpendicularly to the sample surface were recorded at a scattering angle of 160° using a Si(Li) detector with a 15 keV energy resolution. The scatter of the particle energy was sufficiently low to be ignored. The measurement fluence integration was set at 10 μC.

The RBS spectra were modelled using SIMNRA computer code [9]. The modelled surface layer composition was compared with the yttrium profiles generated by SUSPRE code [10].

Results and discussion

Figure 1 presents the atomic concentration of yttrium as a function of implanted fluence for all three kinds of modified steels, as determined by EDX. The Y concentration for 304 and 316L austenitic steels are very similar for all implanted fluences. In both cases, the maximum content of yttrium is about 5 at.% for 5×10^{17} ions/cm^2. A different situation can be observed for 430 ferritic steel. The Y concentration above 5 at.% is obtained already for 1×10^{16} ions/cm^2, a 10 times lower fluence than those for other steels. In 430 substrate, the Y content reaches a maximum value above 6 at.% for the implanted fluence of 1×10^{17} ions/cm^2. For higher implanted fluences, this value saturates.

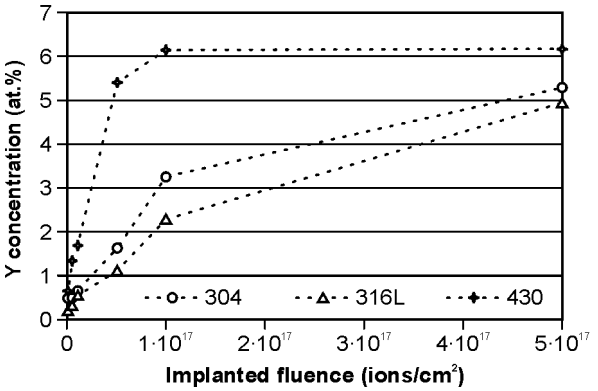

Fig. 1. The Y concentration in 304, 316L and 430 steel after ion implantation as a function of implanted fluence.

The reason of different yttrium accumulations in various steels remains unclear. It may be associated with different crystallographic structures in different steels and/or different yttrium solubilities.

The RBS spectra and the respective profiles of the implanted yttrium are shown in Fig. 2 for all types of substrates and for a fluence of 5×10^{17} ions/cm^2. The upper part shows the virgin spectra of all investigated steels with the appropriately marked positions of steel components. The medium part shows the experimental spectra of yttrium implanted samples with a marked

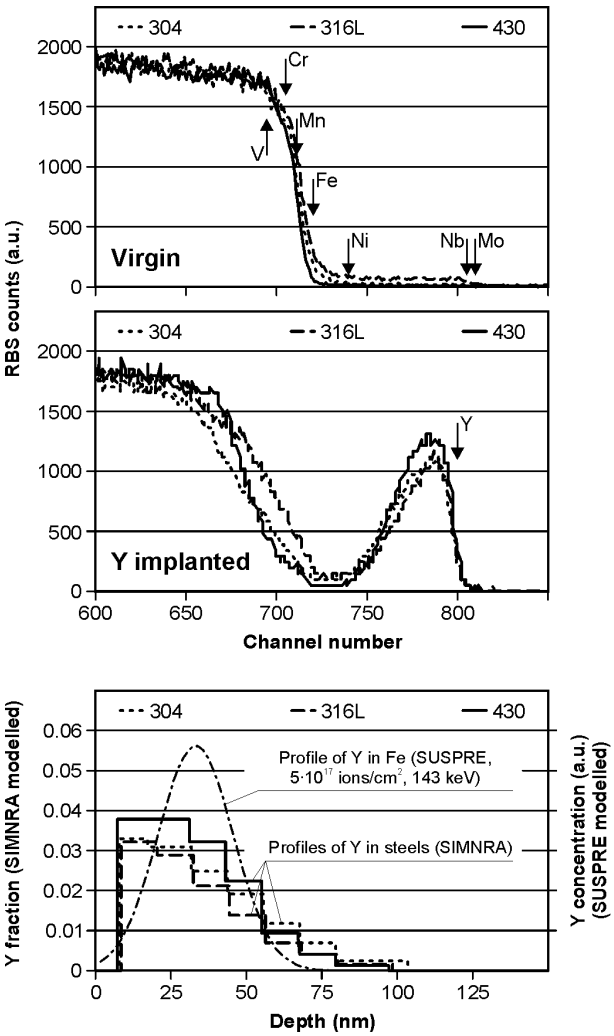

Fig. 2. RBS spectra of different kinds of steel.

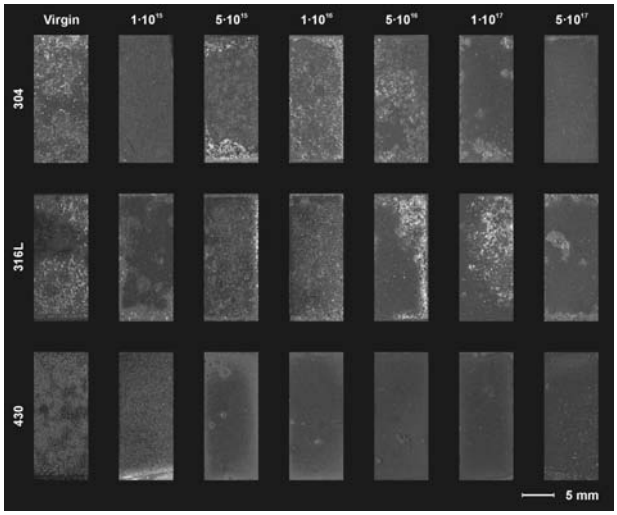

Fig. 3. Microscopic images of 304, 316L and 430 samples for different Y concentrations after high temperature oxidation (1000°C, 100 h).

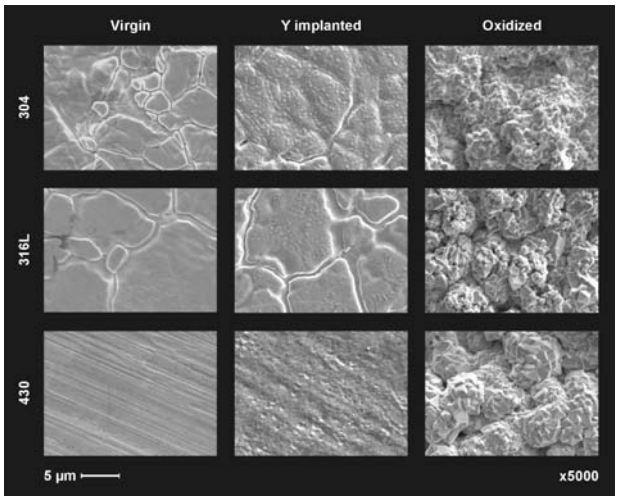

Fig. 4. SEM images of the virgin, yttrium implanted, and oxidized surfaces of different steels for a fluence of 5×10^{17} ions/cm^2.

threshold positions of the implanted species. It may be noticed that yttrium concentrations in all types of steel are comparable.

The lower part shows SIMNRA modelling of the surface layers with the superimposed SUSPRE profile of yttrium in iron. The implantation energy value of 143 keV is the implanter voltage (65 kV) weighted by the yttrium ion average charge (2.2). Due to unavoidable substrate scattering during implantation, the SIMNRA deduced profile is slightly shifted to the surface with respect to the SUSPRE distribution.

The thickness of Y modified layers was similar for all cases. The layers were located at the same depth. The determined profiles were compatible with the Y profile in Fe substrate calculated by the SUSPRE code.

The macroscopic surface images of specimens containing different amounts of yttrium after oxidation in air at 1000°C for 100 h are shown in Fig. 3. The whole surface of the untreated samples were covered by pits and areas of detached scales.

In the case of the modified samples, the visible improvement of surface quality were obtained for implanted fluences 1×10^{17}, 5×10^{17} and 5×10^{17} ions/cm^2 for 304, 316L and 430 steel, respectively. This situation relates to the change of yttrium concentration shown in Fig. 1. Our results are an example of the difference between the behaviour of two types of the investigated steels. It seems that in the case of ferritic steel, to obtain a similar oxidation resistance, the yttrium concentration may be about 100 times lower as compared to the modified austenitic steels. The optimum range of yttrium content is from 5×10^{17} to 1×10^{17} ions/cm^2. According to Fig. 3, we can say that the optimum value of Y concentration in austenitic steels has not been reached.

Figure 4 presents the SEM images of the virgin, yttrium implanted, and oxidized surfaces of different steels for a fluence of 5×10^{17} ions/cm^2. Differences in the nature of untreated surfaces of austenitic and ferritic steels are related to the methods of surface preparation. In the images of implanted surfaces we can see the precipitations of an unknown phase, mainly inside the grains. Changes in the surface nature were the greatest for 430 steel. Nevertheless, the traces of surface preparation of virgin material are still visible. The results of the observation of all the oxidized materials are similar. The sharp-edged and rounded shape grains are observed in each oxidized surface. Similar situation was described in Ref. [19].

Conclusions

The paper confirms previous reports that the ion implantation of yttrium leads to an improvement of high-temperature oxidation resistance of stainless steel. The results of our investigations show that the effectiveness of yttrium implantation for ferritic steel is higher by a factor of about 100 in comparison with austenitic steels. The optimum Y concentration in 430 steel ranges from the implanted fluence of 5×10^{15} to 1×10^{17} ions/cm^2. The optimum value of Y concentration in 304 and 316L steels is unknown. The EDX measurement and results of SEM observation results suggests that this concentration should exceed 5 at.%.

A closer interpretation of the role of yttrium in oxidation processes would require a microscopic study of the fate of yttrium atoms during high temperature processes. In particular, a relation between the implanted atom location and ground boundaries (know a paths of rapid diffusion of metal and oxygen atoms) should be established.

Acknowledgment. The authors wish to thank Mr. J. Zagórski for technical assistance. This work has been supported by the European Community as an Integrating Activity 'Support of Public and Industrial Research Using Ion Beam Technology (SPIRIT)' under EC contract no. 227012.

References

1. Abreu CM, Cristoba MJ, Novoa XR, Pena G, Perez MC, Rodriguez RJ (2002) Modifications of the stainless steels passive film induced by cerium implantation. Surf Coat Technol 158/159:582–587

2. Alman DE, Jablonski PD (2007) Effect of minor elements and a Ce surface treatment on the oxidation behavior of an Fe-22Cr-0.5Mn (Crofer 22 APU) ferritic stainless steel. Int J Hydrogen Energy 32:3743–3753
3. Balland A, Gannon P, Deibert M, Chevalier S, Caboche G, Fontana S (2009) Investigation of La_2O_3 and/or $(Co,Mn)_3O_4$ deposits on Crofer22APU for the SOFC interconnect application. Surf Coat Technol 203:3291–3296
4. Brylewski T, Przybylski K, Morgiel J (2003) Microstructure of Fe-25Cr/(La, Ca)CrO_3 composite interconnector in solid oxide fuel cell operating conditions. Mater Chem Phys 81:434–437
5. Bugaev SP, Nikolaev AG, Oks EM, Schanin PM, Yushkov GY (1994) The "TITAN" ion source. Rev Sci Instrum 65:3119–3125
6. Chevalier S, Bonnet G, Dufour F, Larpin JP (1998) The REE: a way to improve the high-temperature behaviour of stainless steels? Surf Coat Technol 100/101:208–213
7. Cleugh D, Blawert C, Steinbach J, Ferkel H, Mordike BL, Bell T (2001) Effects of rare earth additions on nitriding of EN40B by plasma immersion ion implantation. Surf Coat Technol 142/144:392–396
8. Fontana S, Amendola R, Chevalier S *et al*. (2007) Metallic interconnects for SOFC: Characterisation of corrosion resistance and conductivity evaluation at operating temperature of differently coated alloys. J Power Sources 171:652–662
9. http://home.rzg.mpg.de/~mam/
10. http://www.surrey.ac.uk/ati/ibc/research/modelling_simulation/suspre.htm
11. Jedlinski J, Godlewski K, Mrowec S (1989) The influence of implanted yttrium and cerium on the protective properties of a β-NiAl coating on a nickel-base superalloy. Mater Sci Eng A 120/121:539–543
12. Jedliński J, Mrowec S (1987) The influence of implanted yttrium on the oxidation behaviour of β-NiAl. Mater Sci Eng 87:281–287
13. Lian Y, Qunji X, Wang H (1995) The tribological behaviour of GCr15 bearing steel implanted with cerium. Surf Coat Technol 73:98–104
14. Perez FJ, Otero E, Sierro MP *et al*. (1998) High temperature corrosion protection of austenitic AISI 304 stainless steel by Si, Mo and Ce ion implantation. Surf Coat Technol 108/109:127–131
15. Picardo P, Chevalier S, Molins R *et al*. (2006) Metallic interconnects for SOFC: Characterization of their corrosion resistance in hydrogen/water atmosphere and at the operating temperatures of differently coated metallic alloys. Surf Coat Technol 201:4471–4475
16. Przybylski K (1988) The influence of yttrium on the formation and growth mechanism of chromium oxide layer on scaling-resistant alloys. Stanisław Staszic Academy of Mining and Metallurgy, Kraków (in Polish)
17. Qu W, Li J, Ivey DG (2004) Sol-gel coatings to reduce oxide growth in interconnects used for solid oxide fuel cells. J Power Source 138:162–173
18. Riffard F, Buscail H, Caudron E, Cueff E, Issartel C, Perrir S (2002) Effect of yttrium addition by sol-gel coating and ion implantation on the high temperature oxidation behaviour of the 304 steel. Appl Surf Sci 199:107–122
19. Sartowska B, Piekoszewski J, Walis L *et al*. (2011) Structure and composition of scales formed on AISI 316 L steel alloyed with Ce/La using high intensity plasma pulses after oxidation in 1000°C. Acta Phys Pol A 120:83–86